Computational Methods in Coupled Electron–Ion Monte Carlo Simulations

Carlo Pierleoni*[a] and David M. Ceperley[b]

In the last few years, we have been developing a Monte Carlo simulation method to cope with systems of many electrons and ions in the Born–Oppenheimer approximation: the coupled electron–ion Monte Carlo method (CEIMC). Electronic properties in CEIMC are computed by quantum Monte Carlo rather than by density functional theory (DFT) based techniques. CEIMC can, in principle, overcome some of the limitations of the present DFT-based ab initio dynamical methods. The new method has recently been applied to high-pressure metallic hydrogen. Herein, we present a new sampling algorithm that we have developed in the framework of the reptation quantum Monte Carlo method chosen to sample the electronic degrees of freedom, thereby improving its efficiency. Moreover, we show herein that, at least for the case of metallic hydrogen, variational estimates of the electronic energies lead to an accurate sampling of the proton degrees of freedom.

1. Introduction

Modern theoretical methods in condensed matter physics and chemistry rely heavily on numerical simulations. The problem of solving the Schroedinger equation for many-body systems is too difficult to be addressed directly, even within the simplification provided by the Born–Oppenheimer approximation. In the most popular practical approaches (Hartree–Fock (HF) and density functional theory (DFT) based methods) the original problem is replaced by the problem of solving the time-independent Schroedinger equation for a single electron in the field of the nuclei and the mean field generated by the other electrons.[1] DFT is, in principle, an exact theory but the energy functional must be treated approximately for practical purposes. In the simplest local density approximation (LDA), this exact theory becomes a self-consistent mean field theory. Extensions of LDA, such as the generalized gradient approximation (GGA) provide more accurate results but remain essentially at the level of an effective mean field treatment. Despite the mean field character, DFT schemes have proven to provide quite accurate results for many different systems.[1]

In 1985, Car and Parrinello introduced an efficient method to couple standard molecular dynamics (MD) for classical nuclei with the electronic structure calculation at the level of LDA done "on the fly" to extract the nuclear forces.[2] Because the method allowed the study of the statistical mechanics of classical nuclei with many-body electronic interactions, it opened the way for the use of simulation methods for realistic systems with an accuracy well beyond the limits of the effective force fields available. In the last twenty years, the number of applications of Car–Parrinello ab initio molecular dynamics has ranged from simple, covalently bonded solids, to high-pressure physics, materials science, and biological systems. There have also been extensions of the original algorithm to simulate systems at constant temperature and pressure,[3] finite temperature effects for the electrons,[4] and quantum nuclei.[5]

Despite recent progress, DFT suffers from well-known limitations, for example, excited state properties such as the optical gap and spectra are less reliable. DFT shows serious deficiencies in describing van der Waals' interactions, nonequilibrium geometries such as reaction barriers, and systems with transition metals and/or cluster isomers with competing bonding patterns.[1,6] As a consequence, current ab initio predictions of metallization transition at high pressures, or even predictions of phase transitions, are often only qualitative. Hydrogen is an extreme case,[7–9] but even in silicon the diamond/β–tin transition pressure and the melting temperature are seriously underestimated.[10]

Another route to the ground state properties of a system of many electrons in the presence of nuclei is the quantum Monte Carlo (QMC) method.[6,11] In its simplest form, an analytic many-electron wavefunction is chosen on the basis of the variational principle (variational Monte Carlo, VMC) and the quantum averages are obtained by a Metropolis Monte Carlo simulation of the electronic coordinates. A more accurate representation of the ground-state wavefunction can be obtained by projecting the variational wavefunction with the operator $\exp\{-\beta_e H\}$ where H is the many-body Hamiltonian, and β_e is the projection time. Provided that the variational wavefunction is not orthogonal to the ground-state wavefunction, the projected function tends exponentially fast to the ground-state wavefunction as $\beta_e \rightarrow \infty$. Since matrix elements of the above projection operator at large values of β_e are unknown for nontrivial systems, a Trotter breakup in many (P) small, imaginary time intervals ($\tau_e = \beta_e/P$) must be employed. In the configuration representation, each projection corresponds to a $3N$-dimensional integral that can be performed by the Metropolis Monte Carlo method provided that the propagator in imagina-

[a] *Prof. C. Pierleoni*
Department of Physics, University of L'Aquila
Via Vetoio, 67010 L'Aquila (Italy)
Fax: (+39) 086-243-3033
E-mail: carlo.pierleoni@aquila.infn.it

[b] *Prof. D. M. Ceperley*
Department of Physics and NCSA
University of Illinois at Urbana-Champaign, Urbana, IL 61801 (USA)

 DOI: 10.1002/cphc.200400587

ry time can be chosen real and can be interpreted as a probability distribution. This is the essence of the diffusion Monte Carlo method (DMC), which is an "exact" method for systems of bosons or boltzmannons. This means that all systematic errors in a simulation are under control in the sense that they can be reduced as much as desired. Because electrons are fermions, the above scheme fails because the imaginary time propagator must be completely antisymmetric under exchange of two electrons, and therefore cannot be chosen strictly nonnegative everywhere in configurational space. This is the origin of the infamous "fermion sign problem". In order to avoid the sign problem, the "fixed node approximation" has been proposed and used routinely to perform fermion simulations.[6] The energy calculated with this approximation is variational with respect to the position of the nodal surfaces of the trial wavefunction. Over the years, the level of accuracy of the fixed node approximation for simple homogeneous systems, such as ^{3}He and the electron gas, has been systematically improved by introducing more sophisticated nodal surfaces (backflow orbitals).[12,13] In more complex, inhomogeneous situations such as atoms, molecules, and extended systems of electrons and nuclei, progress has been somewhat slower. Nonetheless, in most cases, fixed-node QMC methods have proven to be more accurate than mean field methods (HF and DFT).[6] Computing ionic forces with QMC to replace the DFT forces in ab initio MD is more difficult, and a general and efficient algorithm is still missing. Moreover, the computer time required for a QMC estimate of the electronic energy is, in general, more than for a corresponding DFT–LDA calculation. These problems have seriously limited the development of an ab initio simulation method based on the QMC solution of the electronic problem "on the fly".

In recent years, we have developed a different strategy based entirely on the Monte Carlo method both for solving the electronic problem and for sampling the ionic configuration space.[14,15] The new method, called the coupled electron–ion Monte Carlo method (CEIMC) has so far been applied to high-pressure metallic hydrogen, where it has found quite different effects of temperature than CPMD based on the LDA forces.[16] Our present interpretation of the disagreement is that LDA provides a Born–Oppenheimer surface smoother than the more accurate QMC one, and this strongly affects the structure of the protonic system at $T>0$.

This paper is organized as follows. Section 2 is devoted to an outline of the CEIMC method. We will not go into all details, since two long articles have appeared on general aspects and early implementations of the method.[14,15] One of the new aspects that we have recently implemented in CEIMC, not described in those references, is the reptation Quantum Monte Carlo (RQMC) projection of the electronic variational wavefunction.[17] So, in Section 2.1, we review the RQMC method and in Section 2.2 we focus on the sampling algorithm: We introduce our new scheme for improving the efficiency and reliability of RQMC, and we provide an analytical proof. In Section 3, we report numerical results on the convergence of the new scheme with the projection time and with the Trotter time step. Finally, in Section 4, we conclude.

2. The Coupled Electron–Ion Monte Carlo Method

The CEIMC method is based on the Born–Oppenheimer (BO) separation between the slow nuclei and the fast electrons. This is in contrast with other quantum Monte Carlo methods, diffusion Monte Carlo[6,11] and finite-temperature path integral Monte Carlo (PIMC)[18,19] methods where electrons and ions are treated on the same footing. As usual, the BO approximation allows the limitations of the other QMC methods to be overcome, while introducing an often negligible error.

In CEIMC, the configurational space of the proton degrees of freedom at inverse temperature $\beta=(k_B T)^{-1}$ is sampled with a Metropolis algorithm in which the difference between the BO energy of a proton state S and of a trial state S' is computed by an electronic ground state QMC calculation. The QMC estimate of the energy difference $\Delta=[E(S')-E(S)]$ has statistical noise which would bias the standard Metropolis algorithm. Unbiased sampling of the proton configurations is achieved by the penalty method, which replaces the energy difference Δ in the acceptance formula by $\Delta+(\beta\sigma_\Delta)^2/2$, where $\sigma_\Delta{}^2$ is the variance of the energy difference.[20] Because $\sigma_\Delta{}^2>0$, the noise always causes extra rejections, but this compensates for "uphill" moves accepted because of a favorable energy fluctuation.

Several methods for computing energy differences in QMC are available.[14,15] A simple and efficient method is to sample the electronic degrees of freedom from a distribution function which is the sum of the electronic distribution functions for the S and S' states (for example, the sum of the square of the trial wavefunctions in VMC). Averages of operators involving electronic degrees of freedom and a single proton configuration, say S, (for instance total energy, variance, etc.) are then computed by correlated sampling.[11,14,15] For the typical size of the proton moves (between 0.01 and 0.5 Å for classical protons, depending on density and temperature) and the typical system size (up to 54 protons) we have investigated, this method is much more efficient than performing two independent electronic calculations for the states S and S'.

In the ground state QMC methods, an electronic trial wavefunction must be chosen according to the physics of the system being studied. For the metallic phase of hydrogen, we have recently developed analytic functions which include backflow and three-body correlations.[21] These wavefunctions are particularly appropriate to CEIMC, because they have accurate energies already at the variational level, they have no adjustable parameters requiring optimization, and their computational cost is much less than using orbitals expanded in the plane wave basis typically used in QMC calculations.[22]

In metallic systems, finite-size effects are large and must be suitably treated. The common procedure is to repeat the calculation for systems of increasing size and extrapolate to the thermodynamic limit, but this is impractical within CEIMC, because it would have to be performed for any proposed protonic step before its acceptance. A much better strategy is to use a twist averaged boundary condition (TABC) which reduces the finite-size error in the energy to the classical $1/N$ behavior.[15,23]

This consists of averaging the energy over the phase that the many-body wavefunction can pick if a single electron wraps around the supercell. This is equivalent to Brillouin zone sampling in the single electron approximation. Within CEIMC it does not cause a large increase in required CPU time/step.

Finally, a recent improvement to the method is the introduction of quantum effects for the protons, which is quite important in high-pressure hydrogen. This is done by developing the thermal density matrix of protonic degrees of freedom on the BO surface in Feynman path integrals.[16,18] A similar technique in the context of the Car–Parrinello method has appeared.[5] We are not going to discuss the last two aspects of the CEIMC. Although the TABC implementation in CEIMC has been described by Ceperley et al.,[15] our implementation of PIMC for proton degrees of freedom in CEIMC will be the subject of a future publication.

2.1. Reptation Quantum Monte Carlo Method

To go beyond VMC electronic energies, we implemented a reptation quantum Monte Carlo algorithm,[17] rather than the diffusion Monte Carlo algorithm. The implementation of the energy difference method is more straightforward in RQMC, and, furthermore, the averages of the observables which do not commute with the Hamiltonian are not biased.

In RQMC, the ground state wavefunction is obtained by constructing an imaginary time path integral for the electronic degrees of freedom. If $|\Psi_0\rangle$ is the trial state, the trial state projected in a "time" $\beta_e/2$, $|\Psi_{\beta e/2}\rangle = e^{-\beta_e H/2}|\Psi_0\rangle$, will converge to the ground state for large β_e. Let us define the "partition" function by Equation (1):

$$Z_{\beta_e} = \langle\Psi_0|e^{-\beta_e H}|\Psi_0\rangle \tag{1}$$

The energy is then defined by Equation (2):

$$E(\beta_e) = -\frac{d}{d\beta_e}\ln Z_{\beta e} = \frac{1}{Z_{\beta e}}\langle\Psi_0|e^{-\beta_e H}H|\Psi_0\rangle = \langle E_L(R)\rangle \tag{2}$$

where the averages of the local energy, $E_L(R) = \Re(\Psi_0^{-1}(R)H\Psi_0(R))$, are with respect to the path average. In practice, the energy is computed as the average of the local energy at the two ends of the path. Here, $\Re$ indicates the real part in the case that the trial function or Hamiltonian is complex. The energy $E(\beta_e)$ is an upper bound to the fixed node energy for each value of β_e; it converges to this at large β_e, and its β_e derivative is strictly negative. This latter quantity is, in fact, minus the variance of the total energy, Equation (3):

$$\sigma^2(\beta_e) = -\frac{dE(\beta_e)}{d\beta_e} = \langle E_L(0)E_L(\beta_e)\rangle - \langle E(\beta_e)\rangle^2 \tag{3}$$

The variance tends to zero for large enough values of β_e, providing a useful signal for the convergence of the energy to the ground state. This is the zero-variance theorem in RQMC. On the other hand, the variance of the local energy computed at either end of the path is the mixed estimator of DMC for $\sigma^2(\beta_e)$. In practical implementations, it is desirable to keep β_e as small as possible, to maximize the efficiency of the energy difference method.

To compute the needed density matrix elements, we divide the projection time β_e into P time slices $\tau_e = \beta_e/P$ and make a semiclassical approximation for $\exp(-\tau_e H)$. Our notation for a single electronic configuration is $R = \{\mathbf{r}_1,\cdots,\mathbf{r}_N\}$, whereas for the entire path it is $s = \{R_0,R_1,\cdots,R_P\}$. The probability distribution for a path is given by Equation (4):

$$\Pi(s) = \exp\left\{-U(R_0) - U(R_P) - \sum_{i=0}^{P-1} L_s(R_{i+1},R_i)\right\} \tag{4}$$

where $U(R) = \Re[\ln\Psi_0(R)]$ and $L_s(R,R')$ is the symmetrized link action for our approximation of the short time propagator. We have used the importance sampling Green's function of the DMC propagator [Eq. (5)]:

$$\langle R|e^{-\tau_e H}|R'\rangle = |\frac{\Psi_0(R)}{\Psi_0(R')}|\exp\left[-\tau_e E_L(R) - \frac{[R'-R-2\lambda\tau_e F(R)]^2}{4\lambda\tau_e}\right] \tag{5}$$

where the force is $F(R) = \nabla U(R)$ and $\lambda = \hbar^2/2m_e$, which provides the symmetrized link action [Eq. (6)]:

$$L_s(R,R') = \frac{\tau_e}{2}[E_L(R) + E_L(R') + \lambda(F^2(R) + F^2(R'))] + \frac{(R-R')^2}{4\lambda\tau_e} + \frac{(R-R')\cdot(F(R)-F(R'))}{2} \tag{6}$$

An alternative form for the link action could be obtained through the pair action developed in the finite temperature path integral MC.[18] However, we have not implemented this form and do not have a comparison of its efficiency.

In order to impose the fixed phase constraint on the projected wavefunction, we must add to the link action a term of the form $L_s^{FP}(R,R') = \lambda\tau_e\int_0^1 d\eta|\nabla\phi(X(\eta))|^2$ where $\phi(X)$ is the phase of the trial wavefunction at electronic position X and the integral is taken over all paths $X(\eta)$ with boundary conditions $X(0) = R$, $X(1) = R'$. We have taken an end-point approximation for this term, except for real wavefunctions in which case fixed-node boundary conditions were used.

Note that in the expressions above, the dependence on the nuclear degrees of freedom was not shown, even though all quantities depend on them. The probability distribution of an electronic path will be $\Pi(s,S)$ where S indicates the position of all nuclei. Because we have an explicit distribution of the electronic paths, it is straightforward to apply the importance sampling scheme for the energy differences by sampling the probability distribution $[\Pi(s,S) + \Pi(s,S')]$ where S and S' are the current and the trial protonic states, respectively. Note also, for VMC $\Pi(s,S) \propto |\Psi_0(s,S)|^2$ becomes the square of modulus of the trial wavefunction (no projection and $R_0 = R_P$).

2.2. The "Bounce" Algorithm

In the original work on RQMC,[17] the electronic path space was sampled by a reptation algorithm, an algorithm introduced to sample the configurational space of linear polymer chains. The

slithering snake or reptation method seems to have originated from the work of Kron[24] and Wall and Mandel.[25] Given a path configuration s, a move is done in two stages. First one of the two ends (either R_0 or R_P) is sampled with probability 1/2 to be the growth end R_g. Then a new point near the growth end is sampled from a Gaussian distribution with a center at $R_g + 2\lambda\tau_e F(R_g)$. In order to keep the number of links on the path-length constant, the old tail position is discarded in the trial move. The move is accepted or rejected with the Metropolis formula, on the basis of the probability of a reverse move. For use in the following, let us define the direction variable d as $d=+1$ for a head move ($R_g=R_P$), and $d=-1$ for a tail move ($R_g=R_0$). In standard reptation, the direction d is chosen randomly at each attempted step.

In the standard reptation algorithm, the transition probability $P(s\rightarrow s')$ is the product of an attempt probability $T_d(s\rightarrow s')$ and an acceptance probability $a_d(s\rightarrow s')$. Note that the path distribution given in Equation (4), because of the symmetrized link action, does not depend on the direction d in which it was constructed. In the Metropolis algorithm, the acceptance probability for the attempted move is given by Equation (7):

$$a_d(s \rightarrow s') = \min\left[1, \frac{\Pi(s')T_{-d}(s' \rightarrow s)}{\Pi(s)T_d(s \rightarrow s')}\right] \tag{7}$$

which ensures that the transition probability $P_d(s\rightarrow s')$ satisfies detailed balance [Eq. (8)]:

$$\Pi(s)P_d(s \rightarrow s') = \Pi(s')P_{-d}(s' \rightarrow s) \tag{8}$$

The autocorrelation time of this algorithm in Monte Carlo steps, that is the number of MC steps between two uncorrelated configurations, scales as $[(\beta_e/\tau_e)^2/A]$, where A is the acceptance rate, an unfavorable scaling for large β_e. Moreover, the occasional appearance of persistent configurations bouncing back and forth without really sampling the configuration space has been previously observed.[26] These are two very unfavorable features, particularly in the present context, where we need to perform many different electronic calculations (at least one per protonic move). There is a premium for a reliable, efficient, and robust algorithm.

We have found that a minimal modification of the reptation algorithm solves both of these problems. The idea is to choose randomly the growth direction at the beginning of the Markov chain, and reverse the direction upon rejection only, the "bounce" algorithm. As far as we are aware, "bounce" dynamics has not been previously investigated for RQMC, though Wall and Mandel[25] mentioned it without a detailed proof and subsequent polymer simulations did not use bounce, perhaps because the acceptance ratio in the polymer systems is much smaller than in RQMC. There is a related algorithm for the directed loop algorithm on the lattice and for simulations of trapped diffusion.[27,28]

What follows is the proof that the bounce algorithm samples the correct probability distribution $\pi(s)$. The variable d is no longer randomly sampled, but, as before, the appropriate move is sampled from the same Gaussian distribution $T_d(s\rightarrow s')$ and accepted according to Equation (7). To be able to use the techniques of Markov chains, we need to enlarge the state space with the direction variable d. In the enlarged configuration space $\{s,d\}$, let us define the transition probability $P(s,d\rightarrow s',d')$ of the Markov chain. The algorithm is a Markov process in the extended path space, and it is as ergodic as a DMC method, hence, it must converge to a unique stationary state, $Y(s,d)$ satisfying the eigenvalue equation [Eq. (9)]:

$$\sum_{s,d} Y(s,d)P(s,d \rightarrow s',d') = Y(s',d') \tag{9}$$

We show that our desired probability $\Pi(s)$ is solution of this equation. Within the imposed rule, not all transitions are allowed, but $P(s,d\rightarrow s',d')\neq 0$ for $d=d'$ and $s\neq s'$ (accepted move), or $d'=-d$ and $s=s'$ (rejected move) only. Without loss of generality, let us assume $d'=+1$, since we have symmetry between ± 1. Equation (9) with $Y(s,d)$ replaced by $\Pi(s)$ is Equation (10):

$$\Pi(s')P(s',-1 \rightarrow s',1) + \sum_{s\neq s'} \Pi(s)P(s,1 \rightarrow s',1) = \Pi(s') \tag{10}$$

Because of the detailed balance of Equation (8), we have $\Pi(s)P(s,1 \rightarrow s',1) = \Pi(s')P(s',-1 \rightarrow s,-1)$, which when substituted in Equation (10) gives Equation (11):

$$\Pi(s')\left[P(s',-1 \rightarrow s',1) + \sum_{s} P(s',-1 \rightarrow s,-1)\right] = \Pi(s') \tag{11}$$

Note that we have completed the sum over s with the term $s=s'$ because its probability vanishes. The term in the bracket exhausts all possibilities for a move from the state $(s',-1)$, thus it adds to one. Hence $\Pi(s)$ is a solution of Equation (9) and by the theory of Markov chains, it is the probability distribution of the stationary state.

3. Results

In order to check the validity of our proof, we first applied the bounce algorithm to an analytically solvable model, namely a one-dimensional harmonic oscillator, and obtained the expected results. For a realistic test, we compare the standard and the bounce algorithms for a fixed pair of protonic configurations (S,S') generated during a VMC run of liquid hydrogen at $T=5000$ K and $r_s=1.31$ [$r_s=(3v/4\pi)^{(1/3)}$, where v is the volume per electron in atomic units]. We have considered $N_p=N_e=16$ protons and electrons using analytic wavefunctions with three-body and backflow terms at the Γ point (periodic boundary conditions).[21] In the test, we fixed the electronic imaginary time step to $\tau_e=0.04H^{-1}$ and the projection time to $\beta_e=0.2H^{-1}$, which corresponds to four links. The key quantity in CEIMC is the correlation time t_c in electronic MC steps of the energy difference $\Delta=E_{BO}(S')-E_{BO}(S)$ which determines, for a fixed length of the electronic run and for a given proton displacement, the noise level. The shorter the correlation time t_c, the larger the number of independent determinations of the energy difference. This implies a smaller noise level and a

larger acceptance for protonic moves, that is, a higher efficiency of the algorithm. In Figure 1 we compare the histogram of the correlation time t_c of the energy difference obtained with standard reptation and with the bounce algorithm over 400 blocks of 10^5 electronic steps. In both calculations, the electronic acceptance rate is 0.89, but the noise level is 0.28 with standard reptation and only 0.14 with the bounce algorithm, in agreement with the observed correlation times. Note that, not only the average, but also the width of the distribution is roughly twice as large with standard reptation than with bounce dynamics.

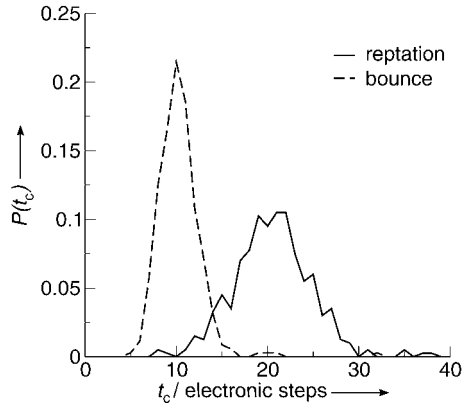

Figure 1. Histogram of the correlation time t_c of the energy difference. Comparison of the reptation and bounce algorithms for a path with four links.

Next, we study the convergence of the bounce algorithm with respect to τ_e and β_e. We first consider protons on a body-centered cubic (bcc) lattice to study the convergence of total energy and variance and to compare with DMC. As above, we consider $N_e = N_p = 16$ at $r_s = 1.31$, with the boundary condition $\theta = 2\pi(0.4,0.5,0.6)$. Data obtained with runs of 10^6 electronic steps are shown in Figure 2. At fixed $\beta = 0.16\,H^{-1}$, we observed a roughly linear convergence (from below) of the total energy with τ_e (not shown). The results in Figure 2 are for $\tau_e = 0.04\,H^{-1}$, which may underestimate the energy by 0.3 mH atom^{-1}. Because of the high quality of the trial function, the ground state was reached with a very small projection time. Already at $\beta_e = 0.6$, the energy saturates at the value obtained with DMC (essentially infinite projection time—shown as a horizontal line in the left panel). The remarkable linear dependence of the energy versus the variance below $\sigma^2 = 0.005$ (right panel) can be used to extrapolate the energy reliably to the $\beta \to \infty$ limit.

In order to study the convergence of the energy difference and to estimate the scaling of t_c with β_e, we consider a pair of successive protonic configurations for the same system generated during a CEIMC run at $T = 5000$ K, that is, in the liquid state. At fixed $\beta_e = 0.16\,H^{-1}$, we study the convergence with τ_e in the range $0.01\,H^{-1} \le \tau_e \le 0.08\,H^{-1}$, and at fixed $\tau_e = 0.02\,H^{-1}$, we study the convergence with β_e in the range $0.08\,H^{-1} \le \beta \le 9.6\,H^{-1}$, which corresponds to $4 \le P \le 480$ time slices. In Figure 3, we show the first two moments $\bar{t}_c$ and σ_c^2 of high-quality Gaussian fits to the histograms of t_c. At fixed β_e, the rejection rate increases linearly with τ_e (not shown). However, successful moves are more effective and this results in the observed scaling $\bar{t}_c \sim \sigma_c \sim \tau_e^{-0.67}$ (left panels) at least in the limited range of values of τ_e spanned. The behavior for increasing β_e at fixed τ_e is more sluggish. Note that the rejection rate, 0.037 in the present case, does not depend on β_e. Both $\bar{t}_c$ and σ_c^2 exhibit a somewhat erratic behavior but the overall scalings are quite favorable. Note that σ_c appears to scale roughly as $\bar{t}_c^2$. Although the quality of the Gaussian fit remains good even at large β_e, for $\beta_e > 1$ the histogram of t_c starts developing a small asymmetry with respect to the maximum with slower decay at large values of t_c.

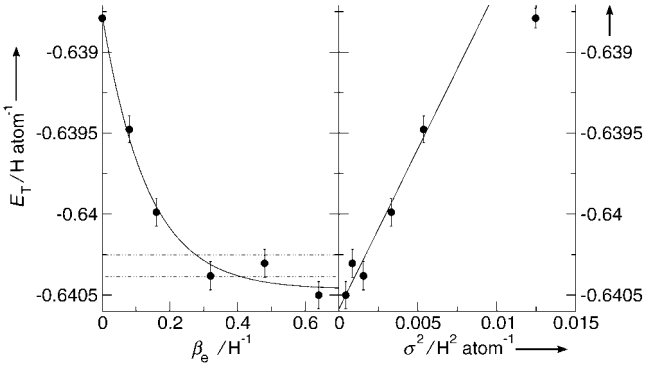

Figure 2. Body-centered cubic hydrogen at $r_s = 1.31$. Convergence with β_e for the energy (left panel) and total energy versus the variance σ^2 (right panel). In the left panel, the curve is a shifted exponential fit; the horizontal dot–dashed lines represent the DMC result with its statistical error.

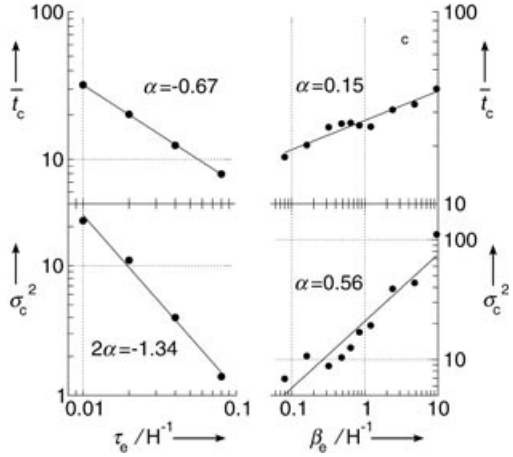

Figure 3. Scaling of the average correlation time $\bar{t}_c$ of the energy difference and of its variance σ_c^2 for a fixed pair of proton configurations. The left panels show the behavior with τ_e at fixed $\beta_e = 0.16\,H^{-1}$; the right panels show the β_e dependence at fixed $\tau_e = 0.02\,H^{-1}$.

In Figure 4, we report the related energy convergence study at fixed $\tau_e = 0.02\,H^{-1}$. In all panels, horizontal lines represent the variational estimate with its statistical error. In particular, Figure 4a shows that the energy difference $\Delta/k_B T$ used in CEIMC to perform the acceptance/rejection test is roughly independent of β_e (neither is there any τ_e dependence at fixed β_e). This result suggests that the difference in the electronic en-

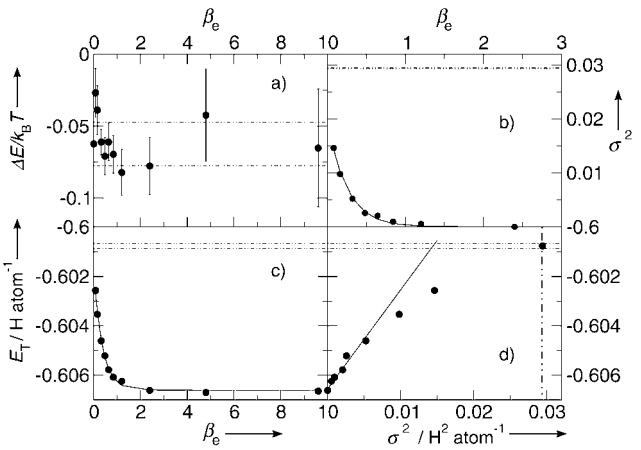

Figure 4. β_e dependence of total energy, variance, and energy difference for a pair of proton configurations (S,S'). The study was performed for $\tau_e = 0.02\,H^{-1}$. Dot–dashed lines represent the variational estimates with their error bars. b,c) The lines are exponential fits to data. d) The continuous line is a linear fit in the region $\sigma^2 \leq 0.005$.

ergies at the variational level is accurate enough to perform CEIMC, at least in the present case of metallic hydrogen with these analytical trial functions; we can sample the proton coordinates using VMC and compute the corrections to the energy and to the equation of state with RQMC for well-equilibrated, statistically independent configurations. From Figure 4c, we see that the projected energy is lower by 5.7 mH atom^{-1} = 1809 K atom^{-1} with respect to the variational estimate, a significant change on the proton energy scale. Figures 4b,c show exponential fits to the data. Figure 4d shows the energy versus the variance. As previously noted, linear behavior is obtained for $\sigma^2 \leq 0.005$.

Finally, in order to test whether the VMC and RQMC computed BO surfaces have the same shape in the relevant part of the proton configurational space and not only at a single point, we studied a system of $N_p = N_e = 54$ atoms at $r_s = 1$ and $T = 1000$ K with zero twist phase (Γ point). A comparison of our VMC pair correlation functions with CPMD–LDA results[29] at this thermodynamic point has recently appeared.[16] The RQMC calculation has been performed with $\tau_e = 0.02\,H^{-1}$ and $\beta_e = 1.0\,H^{-1}$ and provides an energy of $-0.41114(8)$ H atom^{-1} to be compared with the variational estimate of $-0.4087(1)$ H atom^{-1}. The computed pressure is 17.47(1) Mbar and VMC and RQMC estimates are in agreement within error bars. Average correlation time and variance of the energy difference are $\bar{t}_c = 7.1$, $\sigma_c^2 = 2.3$; and $\bar{t}_c = 16.5$, $\sigma_c^2 = 26.5$ for VMC and RQMC respectively. Therefore, going from VMC to RQMC with the same efficiency requires electronic runs between two and three times longer.

4. Conclusions

We have developed a new sampling algorithm for reptation quantum Monte Carlo which we have shown to be more efficient than the standard sampling scheme and to have a favorable scaling with the projection (imaginary) time. This new scheme, which requires a minimal change of existing codes, allows one to sample long electronic paths with a limited effort. We did not observe the occurrence of the pathological situations previously reported with the standard scheme, where the direction was resampled each move. We have implemented the new sampling algorithm in the CEIMC method and found that the correlation time of the energy difference for a given pair of protonic configurations grows like the projection time to the power 0.15. This means, in practice, that the noise level in CEIMC will get only moderately worse with increasing projection time, that is, approaching the ground electronic state. More importantly, we have found that the difference in energy between the two configurations is not sensitive to the projection time, suggesting that CEIMC sampling with VMC provides accurate dynamics. This conjecture has been verified for metallic hydrogen at a single thermodynamic point.

An interesting question that remains unanswered is how general our conclusions are. Since the trial wavefunctions used in the present application are particularly accurate, which is not generally the case, caution must be exercised in applying the algorithms to cases where the accuracy of the trial function is unknown. Aside from this caveat, we do not expect that the method is limited to systems of hydrogen. Heavier elements can be treated either with all their electrons, or using pseudopotentials. How efficient such methods are is an area of active investigation.

Acknowledgements

Early aspects of the CEIMC algorithm were developed in collaboration with M. Dewing. We have pleasure in thanking S. Moroni for useful discussions. This work was supported by a visiting grant from INFM-SezG and by MIUR-COFIN-2003. Computer time was provided by NCSA (Illinois), PSC (Pittsburgh), and CINECA (Italy) through the INFM Parallel Computing initiative.

Keywords: ab initio calculations · high-pressure chemistry · hydrogen · molecular dynamics · theoretical chemistry

[1] R. M. Martin, *Electronic Structure—Basic Theory and Practical Methods*, Cambridge University Press, Cambridge, **2004**.
[2] R. Car, M. Parrinello, *Phys. Rev. Lett.* **1985**, *55*, 2471.
[3] M. Bernasconi, G. L. Chiarotti, P. Focher, S. Scandolo, E. Tosatti, M. Parrinello, *J. Phys. Chem. Solids* **1995**, *56*, 501.
[4] A. Alavi, J. Kohanoff, M. Parrinello, D. Frenkel, *Phys. Rev. Lett.* **1994**, *73*, 2599.
[5] D. Marx, M. Parrinello, *J. Chem. Phys.* **1996**, *104*, 4077.
[6] M. W. C. Foulkes, L. Mitas, R. J. Needs, G. Rajagopal, *Rev. Mod. Phys.* **2001**, *73*, 33.
[7] E. G. Maksimov, Yu. I. Silov, *Phys.-Usp.* **1999**, *42*, 1121.
[8] M. Stadele, R. M. Martin, *Phys. Rev. Lett.* **2000**, *84*, 6070.
[9] K. A. Johnson, N. W. Ashcroft, *Nature* **2000**, *403*, 632.
[10] D. Alfé, M. Gillan, M. D. Towler, R. J. Needs, arXiv: cond-mat/0407038.
[11] B. L. Hammond, W. A. Lester Jr., P. J. Reynolds *Monte Carlo Methods in Ab Initio Quantum Chemistry*, World Scientific, Singapore **1994**.
[12] R. M. Panoff, J. Carlson, *Phys. Rev. Lett.* **1989**, *62*, 1130.
[13] Y. Kwon, D. M. Ceperley, R. M. Martin, *Phys. Rev. B* **1994**, *50*, 1684.
[14] M. Dewing, D. M. Ceperley in *Recent Advances in Quantum Monte Carlo Methods II* (Ed.: S. Rothstein), World Scientific **2002**.

[15] D. M. Ceperley, M. Dewing, C. Pierleoni, *Lecture Notes in Physics*, *Vol.* 605: *Bridging Time Scales—Molecular Simulations for the Next Decade*, Springer-Verlag, Berlin **2003**, pp. 473 – 499.
[16] C. Pierleoni, D. M. Ceperley, M. Holzmann, *Phys. Rev. Lett.* **2004**, *93*, 146402.
[17] S. Baroni, S. Moroni, *Phys. Rev. Lett.* **1999**, *82*, 4745.
[18] D. M. Ceperley, *Rev. Mod. Phys.* **1995**, *67*, 279.
[19] D. M. Ceperley in *Monte Carlo and Molecular Dynamics of Condensed Matter Systems* (Eds.: K. Binder, G. Ciccotti) Editrice Compositori, Bologna, Italy **1996**.
[20] D. M. Ceperley, M. Dewing: *J. Chem. Phys.* **1999**, *110*, 9812.
[21] M. Holzmann, D. M. Ceperley, C. Pierleoni, K. Esler, *Phys. Rev. E* **2003**, *68*, 046707.
[22] a) V. Natoli, R. M. Martin, D. M. Ceperley, *Phys. Rev. Lett.* **1993**, *70*, 1952; b) V. Natoli, R. M. Martin, D. M. Ceperley, *Phys. Rev. Lett.* **1995**, *74*, 1601.
[23] C. Lin, F. H. Zong, D. M. Ceperley, *Phys. Rev. E* **2001**, *64*, 016702.
[24] A. K. Kron, *Polym. Sci. USSR* **1965**, *7*, 1361.
[25] F. T. Wall, F. Mandel, *J. Chem. Phys.* **1975**, *63*, 4592.
[26] S. Moroni, private communication.
[27] L. K. Gallos, P. Argyrakis, K. W. Kehr, *Phys. Rev. E* **2001**, *63*, 021104.
[28] J. K. Anlauf, *Ph.D. Thesis*, University of Cologne **1988**.
[29] a) J. Kohanoff, J. P. Hansen, *Phys. Rev. Lett.* **1995**, *74*, 626; b) J. Kohanoff, J. P. Hansen, *Phys. Rev. E* **1996**, *54*, 768.

Received: December 1, 2004
Published online on ■■ ■■, 2005

ARTICLES

C. Pierleoni, D. M. Ceperley*

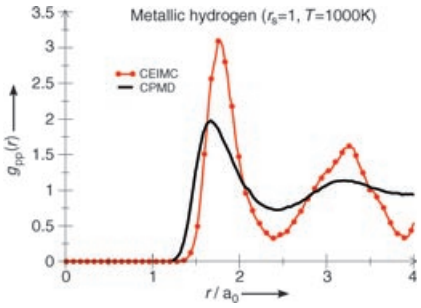

Improving ab initio dynamical simulations: The authors give a detailed description of an efficient reptation quantum Monte Carlo algorithm (coupled electron–ion Monte Carlo method = CEIMC) that they have developed and used to study high-pressure metallic hydrogen (see picture). They observed a large difference in the liquid structure and the liquid–solid transition location with respect to a previous Car–Parrinello molecular dynamics study.